# Wave-based acoustic modeling of the Epidaurus theatre

Konstantinos Kaleris, George Moiragias, Gavriil Kamaris and John Mourjopoulos

Audio & Acoustic Technology Group, Electrical & Computer Engineering Department, University of Patras, Greece.

**Summary**

The acoustics of the ancient theatre of Epidaurus have been evaluated in the past via measurements and models. However, the topic still remains open especially with respect to the contributions of the specific architectural elements to the theatre's excellent acoustic performance. Here, the study focuses on 3 novel aspects for a better understanding of the theater's acoustics: (a) introduces a wave-based acoustics simulation of the Epidaurus theatre based on a flexible but simplified 3D geometric model (b) matches temporal and spectral features of measured and modeled responses, The wave model considers direct, reflected, diffracted and mixed reflection - diffraction sound paths for calculating the theatre's acoustic Impulse Response (IR) in several listening positions, from the front rows of the lower tier to the last rows of the upper tier. For exact tuning of the model, such simulated IR discrete temporal features due to the calculated sound paths are examined through time-distance matching, allowing thus direct comparison to the theatre's measured IRs and further interpretation of the effects of each of the architectural features of the theatre. In order to precisely match the simulation to measurements, the acoustic behavior of reflecting and diffracting surfaces/edges is incorporated in the model through application of special filters, developed according to the spectral characteristics of the reflection and diffraction features of the measured IRs. From the study it is deduced that sound diffraction plays a major role in the theatre's acoustics, assisting signal reception especially at the distant positions.

**PACS no. 43.55.Gx, 43.55.Ka**

## 1. Introduction

The Epidaurus theatre represents the best preserved of the classical Greek-era theatres having remarkable acoustics with renowned speech intelligibility for audiences up to 14500 people. For many years, acousticians have examined the Epidaurus theatre properties [1,2] and many recent acoustic measurements have confirmed perfect intelligibility even for seating positions at 60m from the source (the actors at the “orchestra”), provided that background noise is not excessive. Early computer acoustic simulations of the theatre were performed by Vassilantonopoulos and Mourjopoulos in 2002 [4], which predicted high speech intelligibility and described the paths for the theatre’s early reflections, results that were confirmed in 2004 by detailed measurements for the same source-receiver positions used by the computer model [5,6]. These measurements also revealed a frequency response dominated by a dip at approx. 180 Hz and an amplification of the 500-1500 Hz region. More recently, Declercq and Dekeyser [7] employed a geometric-based acoustic modelling method incorporating multiple orders of diffraction and concluded that the backscattered sound from the cavea amplifies high frequencies more than low frequencies. Farnetali et al. [8] studied open theatre reflection-diffraction effects with measurements both in-situ and in scale models, also indicating the importance of the direct sound, the two early reflections from the floor and stage building (when present) and reflections that correspond exactly to seven step edges behind the microphone position. Additional effects from the ground floor and cavea tier steps specular reflections and edge diffraction was also studied in [9,11]. Lokki et al. [10] developed a model of the lower cavea of the Epidaurus via a 3D finite-difference time domain (FDTD) and a beam tracing method. They illustrated the theatre’s sound field evolution and found that the direct sound and floor reflection from the stage floor are integrated at low frequencies and are combined with the backscattering from the seat rows behind the receiver positions, thus confirming the predictions from earlier studies [8]. They have also shown that the interference of this backscattered sound is responsible for the measured 180Hz dip in the theatre's frequency response [5,6]. The significant of modelling diffraction paths during simulations of the acoustics of the ancient theatres was demonstrated by Economou and Charalambous [18].

Subsequent measurements of the theatre [12,13], confirmed the earlier results for the range of the theatre's acoustic parameters. Especially significant were the detailed measurements of Psarras and Kountouras in 2011 [17] providing novel findings with respect to the effect of audience on the theatre acoustics and their results, taken also at similar positions to the earlier computer simulations, were subsequently combined with the 2004 measurements of Vassilantonopoulos et al. [14]. Surprising finding of the Psarras and Kountouras measurements [17], was the significant reduction in speech intelligibility when the lower tiers of the theatre were covered by plastic seating mats prior to modern-day performances, indicating that the energy reflected and/or diffracted from such geometric elements plays important role in the theatre's acoustic response. Furthermore, the same measurements also indicated that when the theatre is occupied by audience, such additional absorption is not affecting the high intelligibility values. Given that the complex paths in such acoustic transmission effects cannot be detected via usual image and ray-tracing computational methods, here a wave-based simulation [18] of the theatre's acoustics is undertaken, focusing on the detailed evaluation of such reflection / diffraction effects in the receiver position. In order to achieve proper degree of realism, a highly detailed profile for the steps, tiers and cavea slope is introduced, resulting to heavy computational model. For this, the study here is restricted by modelling only a narrow profile strip of the theatre (step/tier width = 60cm) consisting of straight and not curved tiers, hence excluding evaluation of later transmission paths arriving from the sides of the cavea and thus ignoring related effects occurring in the horizontal plane.

The model is finely tuned with respect to the simulated geometry, so that the evaluated impulse response (IR) matches well the measured IR for the same source/receiver positions [6,14]. Then, beyond the evaluation of early reflections, the diffraction paths of different order are isolated and associated to the corresponding physical transmission mechanisms and are successively assessed with respect to their contribution to the theatre's response, its acoustic parameters and the predicted speech intelligibility.

## 2. Description of sound field

From past work [7-11] it is evident that the sound field of open-air amphitheatres is generated via the combination of different reflection, diffraction and propagation mechanisms. Here, such mechanisms – beyond the direct path propagation from source to receiver - are categorized as:

a) reflected paths (r) due to different reflection orders
b) reflected and diffracted paths from a single diffraction point (rd1)
c) reflected and diffracted paths from up to two diffraction points within a path (rd2)
d) reflected, diffracted and diffracted-reflected paths from a single reflection point between two diffraction points (rd2b1)

It is now convenient to include such description in the subsequent analysis of the impulse responses, either from past measurements or derived via acoustic modeling software tools. Hence, the acoustic response of the theatre at a specific listener position $S$ is described by its impulse response $h_S$ at that position which can be expressed as a time domain function constituting of a number of terms due to the responses of the different sound propagation paths:

$$h_S = h_a^0 + \sum_{i=1}^{N_r} r_i + \sum_{j=1}^{N_d} d_j + \sum_{l=1}^{N_{rr}} rr_l + \sum_{k=1}^{N_{dd}} dd_l + \sum_{m=1}^{N_{rd}} rd_m + \sum_{n=1}^{N_{rdr}} drd_n + \cdots \quad (1)$$

where $h_a^0$ denotes here the direct path and $r_i, d_i, rr_i, dd_i, rd, drd$ denote the reflected, diffracted, reflected-reflected, diffracted-diffracted, reflected-diffracted, reflected-diffracted-reflected paths etc. The terms $N_r, N_d$ etc represent the total number of paths reaching the receiver via the specific propagation mechanisms. Considering that each path can be expressed as convolution of the different propagation mechanisms, Equation 1 can be written as:

$$h_S = h_a^0 + \sum_{i=1}^{N_r} h_a^i * h_r + \sum_{j=1}^{N_d} h_a^j * h_d + \\ + \sum_{k=1}^{N_{rr}} h_a^l * h_r * h_r + \sum_{l=1}^{N_{dd}} h_a^l * h_d * h_d + \\ + \sum_{m=1}^{N_{rd}} h_a^k * h_r * h_d + \sum_{n=1}^{N_{rdr}} h_a^m * h_r * h_d * h_r + \cdots \quad (2)$$

where $h_a^p$ the response of sound propagation in air from source to receiver through a specific path p, and $h_r, h_d$ the responses of sound reflection and diffraction. Since Equation 1 is linear, it can be written in the frequency domain as:

$$H_S = H_a^0 + \sum_{i=1}^{N_r} H_a^i H_r + \sum_{j=1}^{N_d} H_a^j H_d + \sum_{l=1}^{N_{rr}} H_a^l H_r^2 + \\ + \sum_{l=1}^{N_{dd}} H_a^l H_d^2 + \sum_{k=1}^{N_{rd}} H_a^k H_r H_d + \sum_{m=1}^{N_{drd}} H_a^m H_d^2 H_r + \cdots \quad (3)$$

Here, for simplicity all paths corresponding to lateral to the receiver propagation, will be ignored and thus, the above response will be furhter seperated into 2 distinct components regarding the direction of arrival: paths arriving at the listener from the front rows (ascending paths) and paths arriving to the listener from the back rows (descending paths). Such simulated sound paths are shown in Figure 1. Specifically, Figure 1a shows the direct path and two reflected paths from a single reflection point. Figure 1b shows a reflected path with two reflection points. Figure 1c shows diffracted paths reaching the receiver from front while Figure 1d shows similar paths reaching the receiver from behind. Figure 1e shows a path with two diffraction points. Finally, Figure 1f and Figure 1g show reflected- diffracted and reflected-diffracted-reflected paths respectively.

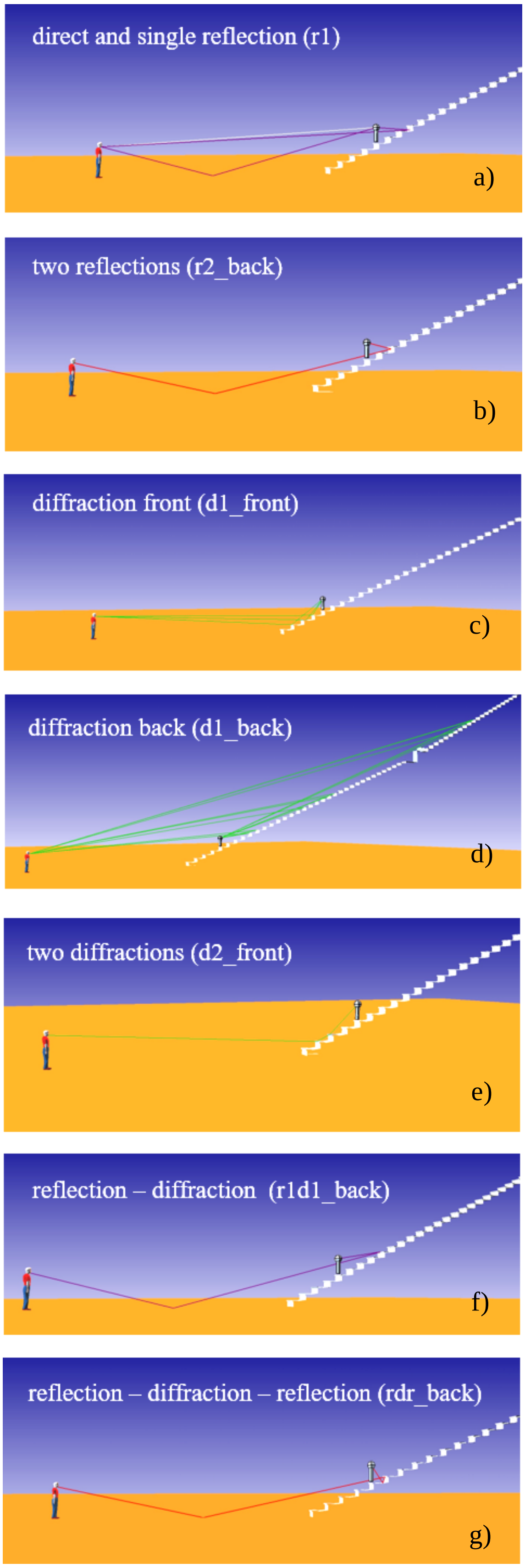


Figure 1. Sound paths from source to receiver including different sound propagation mechanisms: direct (white), diffracted (green), reflected / reflected-diffracted (purple), double reflected / reflected-diffracted-reflected (red)

## 3. Wave-based acoustic model

The wave-based model of the theatre was carried out using the Olive Tree Lab (OTL) software suite [18] for 3D models designed in a dedicated CAD environment. In its Impulse Response calculation engine, OTL uses complex frequency representation of the source signal with parametrized sampling rate and frequency resolution. Wave-based analysis can be performed, considering also sound diffraction (sound

diffraction has been previously investigated in case of Epidaurus [7] and is considered to contribute in the excellent acoustic performance of the theatre). The physics framework of sound reflection / diffraction on a bound surface / edge used for the calculations is given in [19,20].
For this work, two versions of models for the Epidaurus theatre were developed with different levels of detail:

a) a simplified model neglecting the small scale detailed geometric profile of the tier seats, i.e. employing a rough cuboid shape of the tier, see Figure 6a, and
b) a detailed model including exact geometric profile of the tier seats, including the curved surface under the seat's edge and the double sections for the upper side of the seat, see Figure 6b.

For the simulations here, a two-dimensional approximation of the problem was adopted where the theatre cavity is simplified as a strip of straight (not curved) tier rows, considering only horizontal and vertical distances from source while neglecting shifts and propagation on the xy plain. In such case, the sound source emission is transformed from spherical to cylindrical [7], 'though here such consideration is not necessary since the source is placed exactly at the centre of the orchestra. The responses were evaluated in four receiver positions with the following distances from source:

$R1$, lower tier : $(y,z) = (15.30m, 1{,}15m)$
$R4$, lower tier : $(y,z) = (29.70m, 7{,}53m)$
$R7$, upper tier : $(y,z) = (48.10m, 17{,}15m)$
$R10$, upper tier : $(y,z) = (57.50m, 23{,}30m)$

The source was positioned in the centre of the orchestra at $12{,}68m$ distance from the first row at a height of $1{,}485m$. The exact positions of the source and receivers, as well as details of the model's geometry were fine-tuned according to the measured responses presented in [5], see also Section 4.1. In practice, such tuning necessitated to moving the virtual receiver few centimeters either in the horizontal or vertical direction.
As virtual sound source, the "man shouting" parameter included of the Olive Tree Lab library was used. In order to evaluate the effect of varying source level and/or background noise on speech intelligibility (especially with respect to the contributions of the individual response components), the source level was set either to 86dB-SPL / 1m (default) or to 70, 65 and 60 dB-

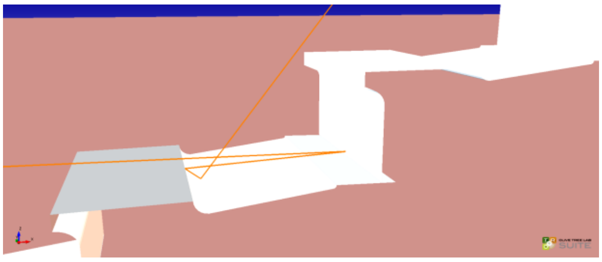

Figure 2. row profile from the detailed model along with complex sound propagation mechanism formed in the cavity of each seat.

SPL. For the Speech Transmission Index (STI) calculations a noise profile according to the NR35 standard was applied, [15,17].
The acoustic responses for the different mechanisms in the various listener positions were evaluated considering the top 60 strongest paths, thus:

$$1 + N_r + N_d + N_{rr} + N_{dd} + N_{rd} + N_{rdr} = 60$$

since it was found that including more paths would not essentially change the results in most cases. It should be noted that especially for the most remote listener positions (R7 and R10) and for the lower source levels, inclusion of more paths (e.g. 200) would improve further the estimated STI. Nevertheless, for reasons of homogeneity all results were extracted for 60 paths.

## 4. Results

### 4.1 Time domain evaluation

The impulse responses presented here were evaluated from the simplified model for reduced computational complexity. However, for the detailed model, were revealed some further propagation mechanisms to the ones shown in Figure 2 for the simplified model. A thorough investigation on such mechanisms should be carried out in the future. For the rd2b1 case, the linear-scale echograms (normalized to the direct signal at position R1) were extracted from the impulse responses at the four listener positions. Figure 3 shows the first $40ms$ of the normalized linear echogram for position R1 (at 15.3m), along with the corresponding measurements [5,15]. Note that any initial delay for the direct path propagation was removed.
The most prominent IR peaks apart from the direct signal are a reflection from the orchestra, reflection from the orchestra and the step back of the row above the listener, along with a reflection from the

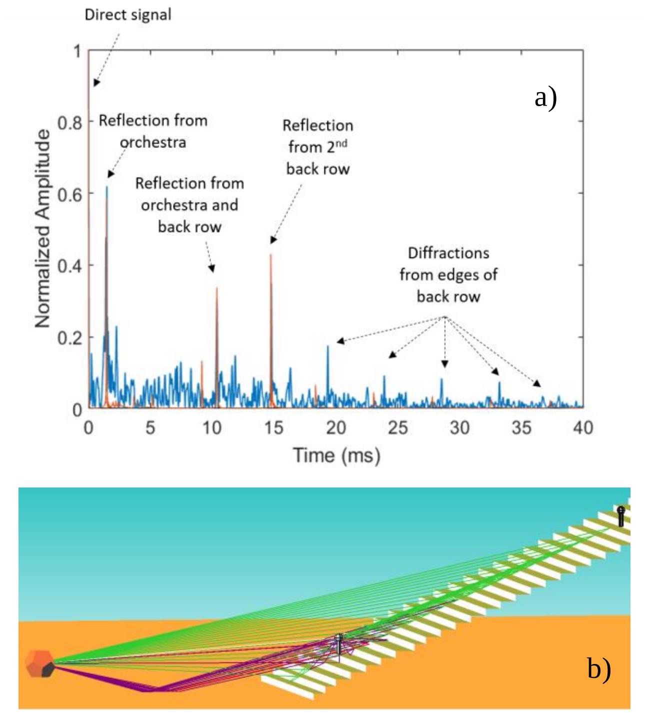


Figure 3. a) simulated (red) and measured (blue) linear echogram at position R1 and b) diagram of the calculated paths.

second row above the listener. Next, the decaying peaks are related to diffracted paths. Here, systematic 1ms drift can be observed in the peak amplitudes between simulation and measurements, which could be related to the approximation of the tier shape via straight sections, hence ignoring any focusing of the acoustic energy in the xy plane due to the theatre's cavity and curved tier shape. Figure 4 shows the linear echogram from the impulse response at position R4 (at 30.6m). Here, the third and fifth peak (apart from the direct path) correspond to a reflected-diffracted-reflected path.
Figure 5 shows the linear echogram of the impulse response at position R7 (at 51.1m). Here it becomes evident that for listener positions at the upper seating area of the theatre, the diffracted energy arrives at shorter intervals after the direct path. The fourth path here is formed by diffraction on the edge of the back 2 rows behind the listener, while the fifth path is a reflection from the back of the listener's row. Significantly, immediately after the reflection from the orchestra, another peak can be identified which differs from the reflected or diffracted peaks in that its energy is spread over longer duration in time. This signal is formed by constructive interference of multiple diffracted paths from different row edges with almost identical travel distances. Such interfering paths are considered to play a major role in the good speech intelligibility of Epidaurus, especially for the more distant listener positions at the mid-higher rows of the upper tier, (see Section 4.3).

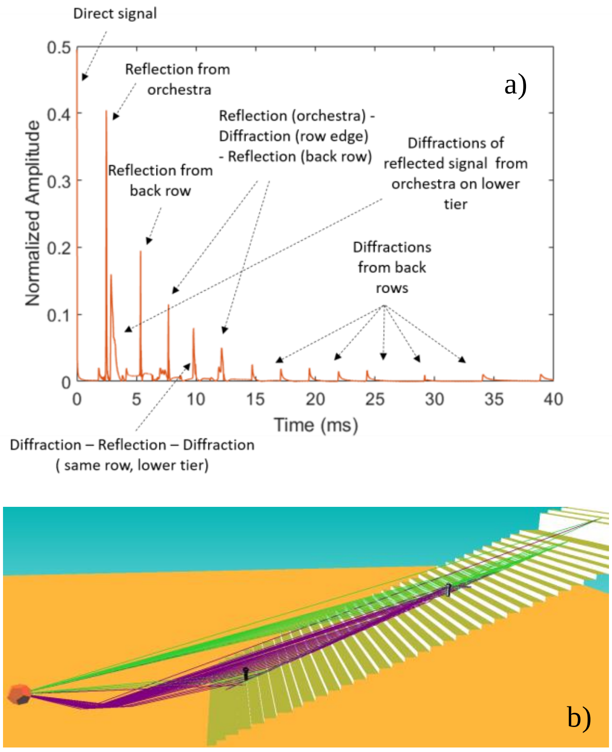


Figure 4. a) simulated linear echogram at position R4 and b) diagram of the calculated paths.

Finally, the linear echogram of the impulse response at the most distant position R10 is shown in Figure 6. Note that this position is at the last row (i.e. there are no potential descending reflections – diffractions). Here, two strong wave fronts are formed from diffracted sound, the first arriving one millisecond after the direct sound and the other one millisecond after the reflection from the orchestra. The first diffracted wave front originates from ascending diffractions of direct signals on the edges of the rows of the upper tier below the listener, while the second from ascending diffractions of the reflected signals from the orchestra on the edges of the lower and the upper tiers, again below the listener position. In the second case, the interference of the diffracted paths seems to lead to the formation of a tail with more than 30ms duration which carries significant low-frequency energy. Such enhancement of low-frequency energy (which also is evident in the corresponding spectra, see Fig.7) might be related to the improvement of the Speech Transmission Index (STI) in the upmost row, observed due to the contribution of diffracted paths, as presented in Section 4.1.

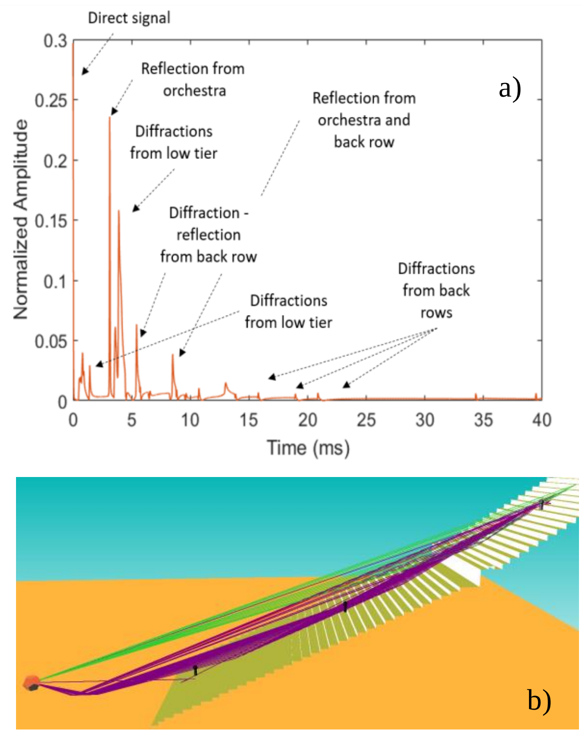


Figure 5. a) simulated linear echogram at position R4 and b) diagram of the calculated paths.

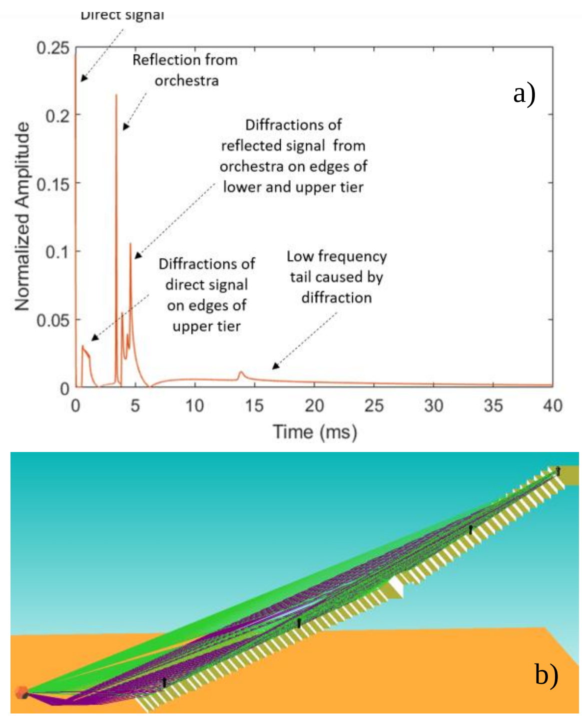


Figure 6. a) simulated linear echogram at position R4 and b) diagram of the calculated paths.

### 4.2 Frequency domain evaluation

From the estimated IRs, the spectra were extracted and a typical (1/10 octave smoothed) spectrum for position R1 calibrated according to the spectrum of the respective measurement (see also Section 4.1) is shown in Fig.7a. From such comparison between measured-simulated spectra, the fine-tuning for optimal spectral matching has been carried out via the absorption coefficients assigned to the surfaces of the orchestra and the tiers in the computer model. Furthermore, it is possible to identify spectral contributions of the reflected and diffracted paths as is shown in Figure 7b for the r and rd2b1 response components. Here it appears that the diffracted paths enhance spectral content in the low and mid frequency range, hence improving SNR at this range and potentially the STI. This observation is also reflected in the Speech Transmission Index values (see Section 4.3).

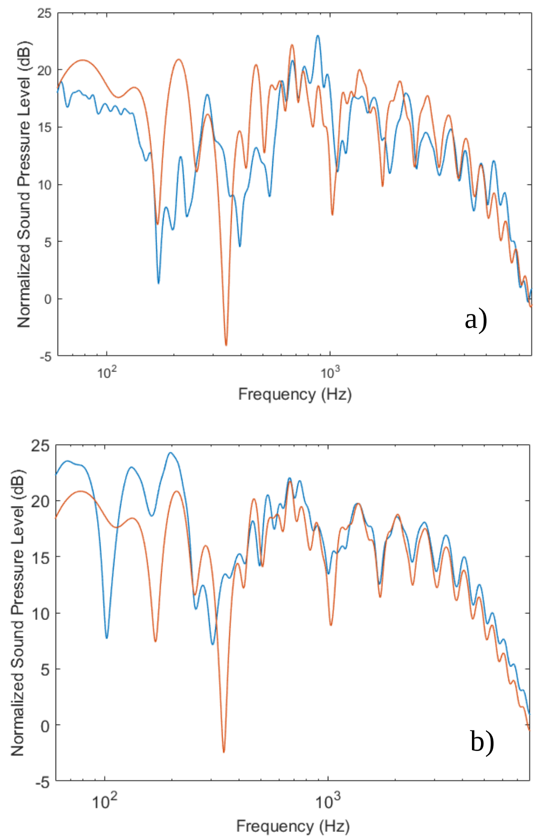


Figure 6. a) Simulated r (red) and measured (blue) spectra and b) simulated r (red) and rd2b1 (blue) spectra

### 4.3 STI

In Table I, the Speech Transmission Index (assuming NR-35 background noise profile) for different source levels is evaluated from the simulated impulse responses for the four listener positions. For each position, the relative STI value when different components of the IR (see Equations 1-3) are taken into account. The STI results indicate a non-negligible contribution of sound diffraction on the speech intelligibility, especially for the upmost listener positions and for weaker source level. Such paths originate mostly from direct or reflected paths from the orchestra that generate ascending diffraction from the edges of the lower rows.

Table I. STI for different source levels and propagation mechanisms

| | | *R1* | *R4* | *R7* | *R10* |
|---|---|---|---|---|---|
| 86dB | *r* | 0.974 | 0.989 | 0.978 | 0.973 |
| | *rd1* | 0.949 | 0.975 | 0.982 | 0.987 |
| | *rd2* | 0.948 | 0.980 | 0.977 | 0.987 |
| | *rd2b1* | 0.960 | 0.979 | 0.986 | 0.988 |
| 70dB | *r* | 0.959 | 0.935 | 0.889 | 0.800 |
| | *rd1* | 0.950 | 0.932 | 0.866 | 0.834 |
| | *rd2* | 0.948 | 0.946 | 0.861 | 0.827 |
| | *rd2b1* | 0.949 | 0.947 | 0.922 | 0.887 |
| 65dB | *r* | 0.922 | 0.901 | 0.733 | 0.673 |
| | *rd1* | 0.931 | 0.849 | 0.753 | 0.692 |
| | *rd2* | 0.929 | 0.865 | 0.752 | 0.686 |
| | *rd2b1* | 0.932 | 0.925 | 0.828 | 0.749 |
| 60dB | *r* | 0.895 | 0.760 | 0.572 | 0.530 |
| | *rd1* | 0.886 | 0.744 | 0.585 | 0.551 |
| | *rd2* | 0.885 | 0.757 | 0.585 | 0.552 |
| | *rd2b1* | 0.862 | 0.787 | 0.669 | 0.612 |

The diffracted sound does not influence significantly the intelligibility for listener positions at the lower rows, where the direct signal and reflections dominate the sound field and hence provide sufficient useful signal. In contrast, such diffracted energy appears to influence positively relatively weak speech signals received at the higher rows, especially at the low frequencies and leading to up to 10% improvement of the overall STI. Such effect was found to allow the STI to exceed the 0.6 threshold of acceptable intelligibility. The per octave band STI for position R10 extracted from the r (reflections only) and rd2b1 impulse responses of the 65dB and 60dB sources is presented in Table II.

Furthermore, it appears that the direction of arrival of the diffracted sound appears to be significant. For the lower positions of the first tier numerous diffracted paths from the edges of the rows behind the listener create a descending sound field, while for the upmost row of the upper tier, diffracted paths combine into a low-frequency ascending wave front reaching the listener from the nearly immediately after the reflection from the orchestra floor, due to the sharper slope angle of these tiers.

### Conclusions

Based on a wave propagation approach, a detailed 2D section of the theatre profile was studied following a precise calibration of the simulation parameters so that fit to measured impulse responses. Here, approximately 60 different paths were found to be sufficient for precise IR and STI estimations.

Such simulation provided a controlled platform to detect and categorise the most important sound propagation mechanisms produced via specular reflections, edge diffraction or their higher order combinations, along with the direction of arrival to receiver (considered here as following an ascending or descending direction).

It was found that the total theatre response is composed from significant diffracted sound field which has non-negligible impact on the theatre's acoustics by enhancing low-mid frequency energy, improving low frequency SNR and appearing to overall STI.

Table II. Per octave band STI at position R10 for different source level

| | | *125Hz* | *250Hz* | *500Hz* | *1kHz* | *2kHz* | *4kHz* | *8kHz* |
|---|---|---|---|---|---|---|---|---|
| 65dB | *r* | 0.224 | 0.429 | 0.542 | 0.667 | 0.768 | 0.796 | 0.712 |
| | *rd2b1* | 0.381 | 0.738 | 0.785 | 0.737 | 0.794 | 0.788 | 0.682 |
| 60dB | *r* | 0.220 | 0.320 | 0.402 | 0.519 | 0.612 | 0.643 | 0.557 |
| | *rd2b1* | 0.274 | 0.585 | 0.634 | 0.588 | 0.655 | 0.666 | 0.561 |

Such diffracted components travel both in an ascending direction (from lower to upper tiers) and descending (form top tiers to the bottom). The ascending components become increasingly significant for the more distant positions in the upper tier, since there, there are no diffractions-reflections coming from behind the listeners. Significantly, at such large distances from the source, the sharper slope of the theatre's upper tier, leads to a concentration of the relative delays of such ascending components towards the direct path and orchestra floor reflection. Furthermore, the total diffracted component is reinforced by the additive effect of the numerous lower tiers. This mechanism can provide a possible explanation for the theatre's near-perfect STI, even at such distant positions.

During these simulated tests, assuming NR=35 noise profile, STI was found to be excellent for a 70dB/1m speaker level and acceptable even for 60dB speaker, in all listening positions.

Future work will examine a more realistic theatre model, incorporating tier curvature and step cavity. The theatre's model performance will be then compared to versions with altered large-scale geometric features (e.g. slope, tier size), or small-scale features (e.g. step profile), to determine their significance to the theatre's unique acoustics.

## Acknowledgement

Konstantinos Kaleris gratefully acknowledges the support of his work by both the General Secretariat for Research and Technology (GSRT) and the Hellenic Foundation for Research and Innovation (HFRI).

## References

[1] F. Canac, "L'acoustique des théâtres antiques", published by the CNRS, Paris, 1967.

[2] R. Shankland, "Acoustics of Greek theatres", Physics Today, pp.30-35, 1973.

[4] S. L.Vassilantonopoulos, J. N. Mourjopoulos, "A Study of Ancient Greek and Roman Theater Acoustics", Acta Acustica united with Acustica, 89, 2002.

[5] S. Vassilantonopoulos, T. Zakynthinos, P. Hatziantoniou, N-A. Tatlas, D. Skarlatos, J. Mourjopoulos, "Measurement and Analysis of Acoustics of Epidaurus Theatre", Hellenic Institute of Acoustics Conference (in Greek), Thessaloniki, 2004.

[6] S. Vassilantonopoulos, P. Hatziantoniou, N-A. Tatlas, D. Skarlatos, J. Mourjopoulos, "Measurement and Analysis of the Acoustics of the ancient theatre of Epidaurus", The Acoustics of Ancient Theatres Conference, 2011.

[7] N.F. Declerq, C.S. Dekeyser, "Acoustic diffraction effects at the Hellenistic amphitheatre of Epidaurus: Seat rows responsible for the marvellous acoustics", J.Acoust.Soc.Am. 121(4), 2007.

[8] A. Farnetani, N. Prodi, R. Pompoli, "On the acoustics of ancient Greek and Roman theatres", J.Acoust.Soc.Am. 124 (3), 2008.

[9] K. Chourmouziadou and J. Kang, "Acoustic evolution of ancient Greek and Roman theatres", Applied Acoustics 69, 514-529, 2008.

[10] T. Lokki, A. Southern, S. Siltanen, L. Savioja, "Studies of Epidaurus with a hybrid room acoustics modelling method", The Acoustics of Ancient Theatres Conference, Patras, 2011.

[11] A. Farnetani, N. Prodi, P.Fausti, "Validation of a numerical code for the edge diffraction by means of acoustical measurements on a scale model of an ancient theatre", The Acoustics of Ancient Theatres Conference, 2011.

[12] K. Angelakis, J. Rindel, A. Gade, "Theatre of the Sanctuary of Asklepios at Epidaurus and the Theatre of Ancient Epidaurus: Objective measurements, computer simulations and listening tests", The Acoustics of Ancient Theatres Conference, Patras, 2011.

[13] G. Cambourakis, A. Sotiropoulou, A.Savvopoulou, G. Poulakos, J.Tzouvadakis, A. Stamos, "Investigations of the Acoustics of the ancient theatre of Epidauros", The Acoustics of Ancient Theatres Conference, Patras, 2011.

[14] S. Psarras, M. Kountouras, "Acoustic and environmental parameter measurements in Epidaurus ancient theatre", The Acoustics of Ancient Theatres Conference, 2011.

[15] S. Psarras, P. Hatziantoniou, M. Kountouras, N.-A. Tatlas, J. N. Mourjopoulos, D. Skarlatos, "Measurements and Analysis of the Epidaurus Ancient Theatre Acoustics", Acta Acustica united with Acustica, Vol.99, 2013.

[16] P. Economou, P. Charalampous, "The Significance of Sound Diffraction Effects in Simulating Acoustics in Ancient Theatres", Acta Acustica united with Acustica, Vol.99, 2013.

[17] N. Hoekstra, B. Nicolai, B. Peeters, C.Hak, R. Wenmaekers, "Project Ancient Acoustics Part 2: Large scale acoustical measurements", ICSV 23, 2016, Athens.

[18] Olive Tree Lab - Suite - The First Integrated Acoustics Software for Indoors and Outdoors." P.E. Mediterranean Acoustics Research & Development Ltd (PEMARD) - Pioneers in Acoustics Software, https://www.mediterraneanacoustics.com/olive-tree-lab-suite.html

[19] Salomons, Erik M. Computational Atmospheric Acoustics. Dordrecht: Kluwer Academic Publishers, 2001.

[20] Hadden, W. James, and Allan D. Pierce. "Sound Diffraction around Screens and Wedges for Arbitrary Point Source Locations'', The Journal of the Acoustical Society of America 71, no. 5 (1982): 1290.